The 14th World Conference on Earthquake Engineering
October 12-17, 2008, Beijing, China

EXPERIMENTAL EVALUATION OF NONSTRUCTURAL COMPONENTS UNDER FULL-SCALE FLOOR MOTIONS

R. Retamales[1], G. Mosqueda[2], A. Filiatrault[3] and A. Reinhorn[4]

[1] *Research Scientist, University at Buffalo, State University of New York, Buffalo, NY, USA, email: rr62@buffalo.edu*
[2] *Assistant Professor, University at Buffalo, State University of New York, Buffalo, NY, USA, email: mosqueda@buffalo.edu*
[3] *Professor, University at Buffalo, State University of New York, Buffalo, NY, USA, email: af36@buffalo.edu*
[4] *C. Furnas Eminent Professor, University at Buffalo, State University of New York, Buffalo, NY, USA, email: reinhorn@buffalo.edu*

ABSTRACT:

In order to better characterize the seismic vulnerability of nonstructural components and equipment and develop effective mitigation measures, the University at Buffalo has commissioned a dedicated Nonstructural Component Simulator (UB-NCS). The UB-NCS is composed of a two-level testing frame capable of simultaneously subjecting displacement and/or acceleration sensitive nonstructural components and systems to realistic full-scale floor motions expected within multistory buildings. The UB-NCS can subject nonstructural components to 3g acceleration, 100 in/s velocity and ±40 in displacement amplitudes. A testing protocol taking full advantage of the new capabilities provided by the UB-NCS has been developed for dynamic testing of acceleration and/or displacement sensitive nonstructural components and distributed nonstructural systems. The protocol motions were applied to assess the seismic performance of a full-scale hospital emergency room containing typical nonstructural components and life support medical equipment and to demonstrate the capabilities of the UB-NCS. The nonstructural components in the emergency room included steel studded gypsum partition walls, suspended ceiling, and a fire extinguishing system. The medical equipment included wall-mounted patient monitors, a ceiling mounted surgical lamp, free standing poles with IV infusion pumps, an operating room video equipment rack, medical gas piping runs inside partition walls, and a crash dummy sitting on a medical gurney. This paper describes the UB-NCS equipment, the proposed testing protocol and the results the nonstructural tests including the seismic performance of individual nonstructural components and medical equipment as well as the dynamic interaction between them.

KEYWORDS: Nonstructural components, seismic fragility, seismic qualification, experimental methods

1. INTRODUCTION

Past earthquakes such as the Northridge earthquake (1994), the Kobe earthquake (1995), and more recently, the Hawaii earthquake (2006), have devastated the world for centuries, affecting both engineered and non-engineered infrastructure. In light of these disasters, many cases of partial or global collapse of major and minor structural systems were observed, and many more cases involving loss of functionality of critical facilities and essential lifelines proved to be devastating. The Northridge earthquake, for example, caused severe damage, disrupting the normal operation of ten hospitals in Los Angeles County. These disruptions were caused by severe structural damage and/or by the failure of nonstructural components like mechanical equipment, elevators and water supply systems (McGavin and Patrucco 1994). The limited data collected from past earthquakes and the relatively limited research dealing with nonstructural components are insufficient to completely characterize their seismic behavior, develop effective mitigation measures, and provide appropriate design guidelines. To address these limitations, the Structural Engineering and Earthquake Simulation Laboratory (SEESL) at the University at Buffalo has commissioned a dedicated Nonstructural Component Simulator (UB-NCS) composed of a two-level testing frame capable of simultaneously subjecting in real-time full-scale displacement and/or acceleration sensitive nonstructural systems and equipment to realistic full-scale floor motions expected at the upper levels of multistory buildings. The input motions for the UB-NCS can be

obtained from the simulated or recorded response of multistory buildings. However, in order to more broadly assess the seismic performance of general nonstructural systems and equipment, independent of building and ground motion, a testing protocol simultaneously applying expected absolute accelerations and story drifts has been developed. The actual testing capabilities and limitations of the UB-NCS, and the suitability of the proposed testing protocol, have been evaluated following an extensive series of tests aiming to evaluate the seismic performance of a full-scale hospital emergency room containing typical nonstructural components and life support medical equipment. The results obtained from the tests performed using the testing protocol have been compared to results observed in tests performed using simulated building floor motions (Retamales 2008).

2. THE NONSTRUCTURAL COMPONENT SIMULATOR (UB-NCS)

The UB-NCS, shown in Figure 1, provides the unique capability to replicate, under controlled laboratory conditions, the effects of strong seismic shaking on distributed nonstructural components located at the upper levels of multistory buildings. Furthermore, the testing equipment allows for assessing the seismic interactions between displacement and acceleration sensitive nonstructural components, providing a more realistic procedure for the seismic qualification of nonstructural systems, as required by current seismic regulations (e.g., 2006 IBC and the SB1953 legislation for hospitals in California). The UB-NCS testing facility can subject nonstructural components and systems to accelerations of up to 3g, peak velocities of 100 in/s and displacements in the range of ±40 in., enveloping the peak seismic responses recorded at the upper levels of multistory buildings during historical earthquakes. The testing frame is activated by four identical high performance dynamic actuators with a load capacity of 22 kips. The frame is composed of two square 12.5 ft platforms with an interstory height of 12 ft in the bottom level and 14 ft in the upper level, as shown in Figure 2. A more detailed description of the testing frame can be found in Mosqueda et al. (2008).

3. PROPOSED TESTING PROTOCOL

Testing protocols currently used for the seismic performance assessment of nonstructural components and equipment (FEMA 2006, ICC-ES 2007) focus either on displacement or acceleration sensitive components, through quasi-static racking or shake table protocols. However, some nonstructural systems may be sensitive to both displacement and accelerations. Further, nonstructural systems typically found in buildings may be composed of components that individually may be either acceleration or displacement sensitive, but when combined with other systems may become sensitive to both accelerations and interstory drifts. In hospitals, for example, acceleration sensitive patient monitors are typically attached to displacement sensitive partition walls. The seismic performance of individual nonstructural components and the assessment of interactions between components can be evaluated through a testing protocol taking full advantage of the UB-NCS capabilities. To this end, an innovative dynamic testing protocol applicable for both experimental seismic fragility assessment and seismic qualification of acceleration and/or displacement sensitive nonstructural systems is proposed. The testing protocol was mainly developed for use with the UB-NCS; nevertheless, the methodology can be used for experimental seismic fragility research on acceleration sensitive components performed using conventional shake table simulators. Previous research by Wilcoski et al. (1997) and Krawinkler et al. (2000) constitutes the basis for the development of this testing protocol.

3.1. Building model and estimation of seismic demands

The proposed protocol consists of a pair of displacement histories for the bottom and top levels of the UB-NCS that simultaneously match: (i) a target Floor Response Spectrum (FRS), and (ii) a target Generalized Interstory Drift (GID), both specified at a given normalized building height h/H, where h is the height above grade where the nonstructural component is located, and H is the total height of the building. The continuous beam model shown in Figure 3 was considered to model a generic multistory building and to describe the seismic load path traveling from the ground to nonstructural components. The building model consists of a continuous elastic cantilever beam combining a flexural and a shear beams connected by an infinite number of axially rigid links distributed along height, allowing for modeling of generic buildings whose seismic resistant systems are composed by either shear walls, moment resistant frames or a combination of both. This model has been

extensively studied by other researchers (e.g. Iwan 1997, Chopra and Chintanapakdee 2001, Kim and Collins 2002, Miranda and Akkar 2006), and has shown promising results in simulating the seismic responses observed in multistory buildings during real ground motions (e.g. Taghavi and Miranda 2006). The parameter α (Figure 3) accounts for the relative stiffness of the shear and flexural beams.

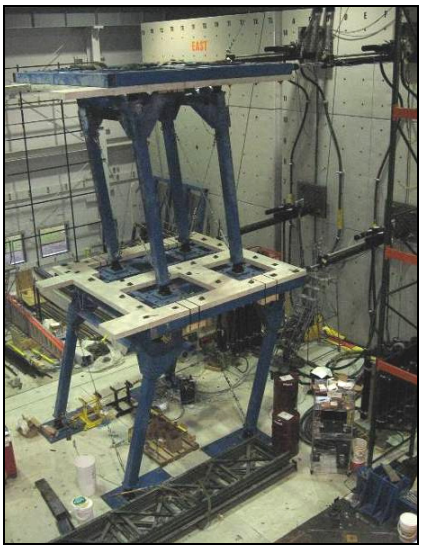

Figure 1. Photograph of the UB-NCS

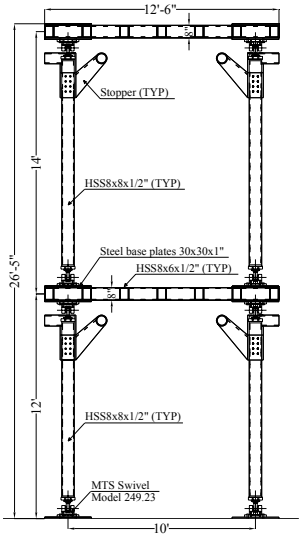

Figure 2. Elevation UB-NCS

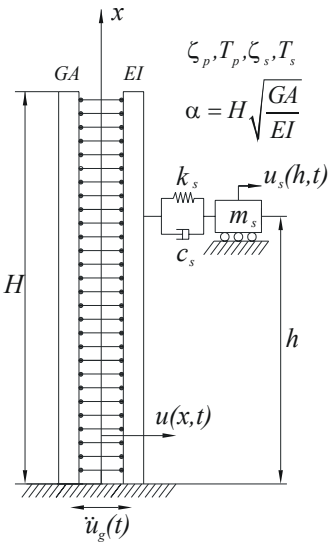

Figure 3. Building model

The input ground motion for the building model is characterized by a Power Spectral Density Function (PSDF), $S_{\ddot{u}_g}(\omega)$, compatible with a Probabilistic Local Seismic Hazard (PLSH) (Gupta and Trifunac 1998). Input/output PSDF relations for the combined primary/secondary system were derived using principles of stochastic processes. The PSDF for the absolute accelerations along the height of the building model, $S_{\ddot{u}^T}(x,\omega)$, the absolute acceleration of a SDOF secondary system located at a height h, $S_{\ddot{u}_s^T}(h,\omega,\omega_s)$, and the generalized interstory drifts, $S_\theta(x,\omega)$, are expressed as follows:

$$S_{\ddot{u}^T}(x,\omega)=\begin{cases} S_{\ddot{u}_g}(\omega)-2S_{\ddot{u}_g}(\omega)\sum_{n=1}^{N_m}\gamma_n\varphi_n(x)\left[1+H_n(\omega)\left(\omega_n^2+2i\zeta_n\omega\omega_n\right)\right]+\cdots \\ S_{\ddot{u}_g}(\omega)\sum_{n=1}^{N_m}\sum_{m=1}^{N_m}\gamma_n\gamma_m\varphi_n(x)\varphi_m(x)\left[1-2H_n(\omega)\left(\omega_n^2+2i\zeta_n\omega\omega_n\right)\right]+\cdots \\ \sum_{n=1}^{N_m}\sum_{m=1}^{N_m}\gamma_n\gamma_m\varphi_n(x)\varphi_m(x)\omega_n\omega_m\left[\omega_n\omega_m+4\zeta_n\zeta_m+2i\omega\left(\omega_m\zeta_n-\omega_n\zeta_m\right)\right]S_{\ddot{u}_g}(\omega)H_n(\omega)H_m^*(\omega) \end{cases} \tag{3.1}$$

$$S_{\ddot{u}_s^T}(h,\omega,\omega_s)=S_{\ddot{u}^T}(h,\omega)\left(4\zeta_s^2\omega_s^2\omega^2+\omega_s^4\right)H_s(\omega)H_s^*(\omega) \tag{3.2}$$

$$S_\theta(x,\omega)=S_{\ddot{u}_g}(\omega)\sum_{n=1}^{N_m}\sum_{m=1}^{N_m}\gamma_n\gamma_m\frac{d\varphi_n}{dx}(x)\frac{d\varphi_m}{dx}(x)H_n(\omega)H_m^*(\omega) \tag{3.3}$$

In Eqns. 3.1, 3.2 and 3.3, $H_s(\omega)=\left(\omega_s^2-\omega^2+2i\zeta_s\omega\omega_s\right)^{-1}$, ω_s and ζ_s denote frequency response function, natural frequency and damping ratio for the secondary system, respectively; $H_n(\omega)=\left(\omega_n^2-\omega^2+2i\zeta_n\omega\omega_n\right)^{-1}$, ω_n, ζ_n, γ_n, and φ_n denote frequency response function, natural frequency, damping ratio, modal participation factor and modal shape for the n^{th} vibration mode of the primary system, respectively. i denotes the imaginary unit and N_m is the number of modes considered in the analysis. Principles of random vibration theory were used to estimate the mean peak seismic demands expected on nonstructural components (Cartwright and Longuet-Higgins 1956).

In developing and calibrating the testing protocol, a PLSH given by a USGS Uniform Seismic Hazard (USH)

ground response spectrum with a probability of exceedance of 10% in 50 years for a region of high seismicity such as Northridge (longitude 118.518 W, latitude 34.237 N), California, was considered. Buildings with deformation patterns defined by parameters $\alpha = 0$, 5 and 10, primary systems with fundamental periods T_p in the range 0.1 to 5 sec, and secondary systems with natural periods T_s in the range 0 to 5 sec, were considered. The damping ratio for primary (all modes) and secondary systems is assumed equal to 5%. N_m=10 modes are considered in the analysis. Figure 4 shows a typical three dimensional Floor Response Spectra (FRS) obtained using Eqns. 3.1 and 3.2 for the case $\alpha = 5$ at building roof level. Note that the dominant amplification occurs when $T_s = T_p$ or T_s is in the range of the predominant ground motion period. Similar 3D FRS's are obtained for the other building heights and α values. The data in Figure 4 and that obtained for other α's have been statistically processed to obtain the expected floor demands that will be applied by the general testing protocol, independent of building deformation pattern α and primary system fundamental period T_p. In order to do so, the mean (over α) 84th % (over T_p) FRS's were computed as functions of normalized building height. The results of this statistical analysis are shown in Figure 5a. A function $FRS_{Factor}(h/H)$, calculated as the quotient between the peak value of the mean 84th% FRS's along the height of the building and the peak spectral amplitude of the PLSH ground response spectrum, is used to amplify the platform motions and to obtain the test target FRS. The best fit curve for the $FRS_{Factor}(h/H)$, shown in Figure 5b, is given by:

$$FRS_{Factor}\left(\frac{h}{H}\right) = 1 + 10\frac{h}{H} - 19.4\left(\frac{h}{H}\right)^2 + 12.4\left(\frac{h}{H}\right)^3 \tag{3.4}$$

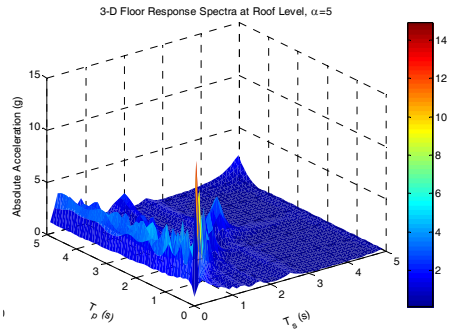

Figure 4. Example of 3D-FRS for α =5, roof level (h/H=1)

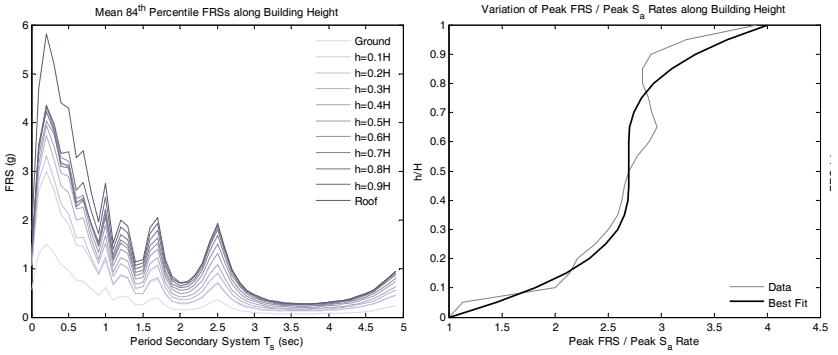

(a) (b)

Figure 5. (a) Mean 84th percentile FRS along building height; and (b) Floor response spectra extrapolation factor

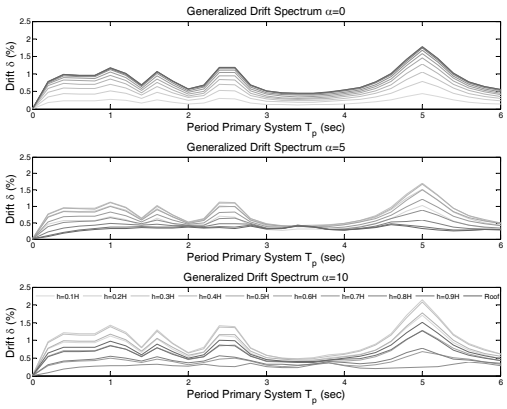

Figure 6. GDS at several building heights

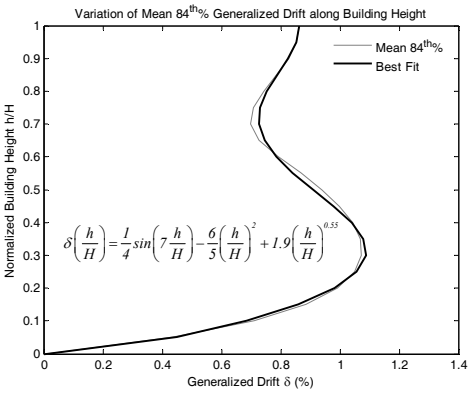

Figure 7. Mean 84th % GID

Using Eqn. 3.3, the PSDF for generalized interstory drifts (GID) were calculated. Principles of stochastic processes were used to compute the generalized drift spectra (GDS) shown in Figure 6. To make the testing protocol independent of deformation patterns and dynamic properties of the primary system, the mean (over α) 84th % (over T_p) GID along building height were determined. Figure 7 shows the mean 84th% GID and its best fit

along building height, given by:

$$\delta\left(\frac{h}{H}\right)=\frac{1}{4}sin\left(7\frac{h}{H}\right)-\frac{6}{5}\left(\frac{h}{H}\right)^{2}+1.9\left(\frac{h}{H}\right)^{0.55}\ \% \tag{3.5}$$

3.2. Generation of hazard consistent floor displacement histories

After computing the demands to be imposed by the testing protocol, displacement histories for the bottom and top levels of the UB-NCS are generated. The key parameters for the protocol histories are the location of the component along the normalized building height and the target uniform seismic hazard. The frequency content targeted for the testing protocol covers the range between f_{min} =0.2 and f_{max} =5 Hz, which corresponds to the UB-NCS operating frequency range. This frequency range is sufficient to capture the first few modes in the responses of multistory buildings. The instantaneous frequency $f(t)$ considered in the protocol is given by:

$$f(t)=f_{max}\left(\frac{f_{min}}{f_{max}}\right)^{\left|\frac{|t-t_d|}{t_d}-1\right|} \tag{3.6}$$

where $t_d=\frac{1}{S_r}log_2\frac{f_{max}}{f_{min}}$ is the time at which the minimum testing frequency is reached. S_r denotes a constant sweep rate calibrated to induce the same number of "Rainflow" cycles (ASTM 1997) on acceleration sensitive nonstructural components as would be experienced during real floor motions. Eqn. 3.6 corresponds to an instantaneous testing frequency transitioning from high to low frequencies, then back to high frequencies. The final high frequency sweep is intended to capture possible high frequency acceleration-induced mode of failures of nonstructural components damaged by low frequency inter-story drifts. The displacement protocol proposed for the UB-NCS bottom level, x_{Bottom}, matches the mean 84th % FRS expected at a given normalized height. The closed-form equation for the bottom level protocol is:

$$x_{Bottom}\left(t,\frac{h}{H}\right)=\bar{\alpha}f(t)^{\beta}cos\left(\varphi(t)\right)w(t)FRS_{Factor}\left(\frac{h}{H}\right) \tag{3.7}$$

where $\bar{\alpha}$=0.75 and β=-1.35 are calibration factors used to minimize the error in matching the ground response spectrum in the range of frequencies of interest; $\varphi(t)$ is the instantaneous phase; and $w(t)$ is a sinusoidal windowing function used to smooth the ramp-up and ramp-down portions of the protocol. The interstory drift protocol is calibrated to impose a controlled number of rainflow cycles on drift sensitive nonstructural components. The peak interstory drift reached during testing matches the mean 84th % GID expected at a given normalized building height. The closed-form equation for the interstory drift protocol, Δ, is given by:

$$\Delta\left(t,\frac{h}{H}\right)=h_{NCS}e^{-\left(\frac{t-t_d}{\sigma}\right)^2}\delta\left(\frac{h}{H}\right)cos\left(\varphi(t)\right)w(t) \tag{3.8}$$

where $\delta(h/H)$ is given in Eqn. 3.5; h_{NCS} is the free interstory height of the UB-NCS; and $e^{-((t-t_d)/\sigma)^2}$ is a Gaussian-shaped modulating function in which σ is calibrated to control the amplitude of the rainflow cycles imposed by the interstory drift protocol. The closed-form equation for the top level protocol, x_{Top}, is given by:

$$x_{Top}\left(t,\frac{h}{H}\right)=x_{Bottom}\left(t,\frac{h}{H}\right)+\Delta\left(t,\frac{h}{H}\right) \tag{3.9}$$

Figure 8 shows the proposed protocol histories for the bottom and top UB-NCS levels for a normalized building

height h/H =1, corresponding to a generic building roof level. Details regarding the calibration of the UB-NCS testing protocol to induce and impose a controlled number of rainflow cycles on acceleration and drift sensitive nonstructural components can be found in Retamales (2008).

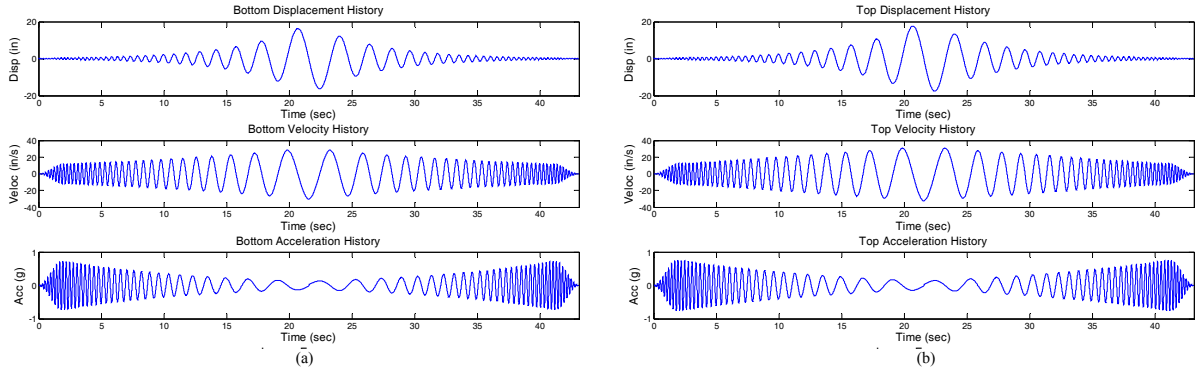

Figure 8. Testing protocol at h/H =1 for (a) Bottom UB-NCS level; and (b) Top UB-NCS level

4. SEISMIC PERFORMACE OF A FULL-SCALE HOSPITAL EMERGENCY ROOM

Experiments were conducted on the full-scale hospital emergency room (ER) replica shown in Figure 9 subjected to full-scale floor motions. The room was constructed following standard hospital construction techniques. The nonstructural partition wall layout was based on a similar specimen tested by Lang and Restrepo (2006). The walls were constructed between concrete slabs attached to the frame (Figure 1). The room was approximately 14.5 ft in length, 10.5 ft in width, and 12.5 ft in height (Figure 10). The simulated ER was furnished with medical equipment critical for inpatients' life support (Figure 11). Medical equipment found in other hospital's critical services was also considered. The nonstructural components and systems, along with the medical equipment, included steel studded gypsum partition walls; lay-in suspended ceilings; fire extinguishing pipe runs (Figure 12e) spanning between the two UB-NCS levels, with a sprinkler head interacting with the ceiling and pipe runs attached to partition walls and top slab; medical gas runs with in-wall outlets (Figure 12b); wall-mounted patient monitors (Figures 12a, 12b); freestanding poles with IV infusion pumps (Figure 12a); ceiling mounted surgical lamp (Figure 12d); operating room video rack on casters (Figures 12a, 16c); medical cart (Figure 12a); and a 180 lb crash dummy sitting on a medical gurney (Figure 12a).

Figure 9. Photo ER

Figure 10. Lateral view ER

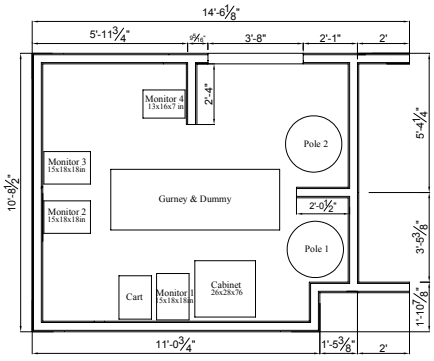

Figure 11. Layout ER

The testing protocol described in Section 3 was used for evaluating the performance of the fully-equipped ER. For fragility analysis purposes the protocol was applied using increasing scaling amplitude factors of 25, 50, 100 and 150%. In addition, to validate the suitability of the protocol to impose earthquake compatible damage levels, the specimen was subjected to the floor motions obtained from the simulated nonlinear response of an existing four story steel framed medical facility located in the San Fernando Valley, California (Wanitkorkul and Filiatrault 2005).

(a) (b) (c) (d) (e)

Figure 12. (a) Dummy sitting on gurney, poles with IV pumps, video rack, cart and monitor; (b) Medical gas piping outlets and monitor; (c) Video rack; (d) Surgical lamp; and (e) Sprinkler runs

During the tests performed considering the testing protocol scaled to 25 and 50% only minor damage was observed. Some hairlines cracks along corner beads and paper joint tape, rising of screws along top and bottom tracks and an incipient diagonal crack at the door fenestration were observed. During the test at 100% of the testing protocol (design earthquake level), at which a peak floor acceleration of 0.77g and a peak interstory drift of 0.87% were reached, more extensive damage was observed. Cracks were observed along corner beads and joints between gypsum panels. The number of raised screws increased. Two monitors attached to the partition walls perpendicular to the direction of loading broke off their mounting systems and the monitor shown in Figure 12b moved out of its supporting system's retention clip (without falling), the large light in the surgical lamp shown in Figure 12d broke off its support after exhibiting excessive displacement and hitting the UB-NCS columns several times. One of the drop-in devices attaching the medical gas piping hangers to the top concrete slab was pulled out from the concrete. The gurney exhibited excessive motion after deactivation of the breaking system and the crash test dummy was thrown off the gurney. Severe impact was observed between the video cabinet and the patient monitor shown in Figure 12a.

During the test for 150% of the testing protocol (maximum considered earthquake level), an even more severe damage was observed. Extensive residual crack openings (~1/8-1/4") were observed along corner beads and joints between gypsum panels. Evidences of rocking of screws attaching gypsum panels to the steel stud frame were observed. The crack in the corner of the door opening propagated. The monitor shown in Figure 12b fell down at this intensity (it was repositioned following the 100% level test). Noticeable residual deformations were observed in the medical gas pipes. Once again, the gurney exhibited excessive motion after deactivation of the breaking system and the dummy was thrown off and almost out of the room. All medical supplies on the medical cart shown in Figure 12a fell down. No damage was observed in the sprinkler system. Figure 13 through Figure 15 show some typical results obtained from experimentation. Figure 13 compares desired and observed interstory drift histories, Figure 14 shows observed FRS's at bottom and upper UB-NCS levels, and Figure 15 shows the ensemble of the hysteresis loops observed during testing.

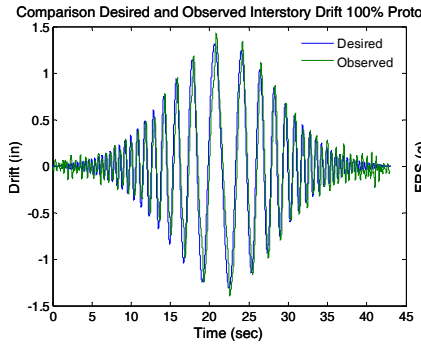

Figure 13. Desired and observed interstory drifts histories

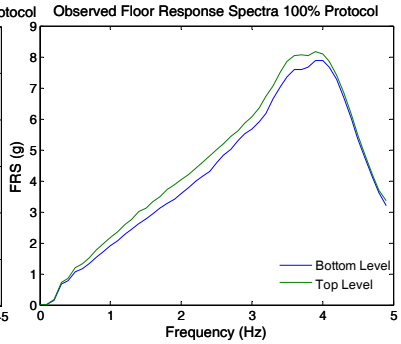

Figure 14. Observed FRS's

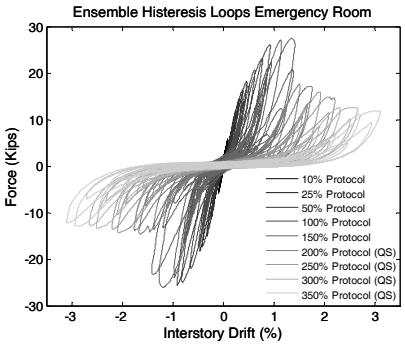

Figure 15. Observed hysteresis loops

Comparable damage in acceleration sensitive components was observed following the tests performed using the simulated building floor motions for the aforementioned medical facility (Retamales 2008). Damage in displacement sensitive components could not be compared due to the preexisting damage in the specimen.

5. CONCLUSIONS

An innovative testing apparatus and testing protocol have been developed for real-time experimental seismic qualification and fragility assessment of full-scale distributed nonstructural systems. The testing frame provides the unique laboratory capabilities to replicate full-scale floor motions expected at the upper levels of multistory buildings, allowing for the simultaneous testing of displacement and/or acceleration sensitive building nonstructural systems and equipment. Further, the seismic interaction between components can be evaluated. The proposed testing protocol can be expressed in closed-form for consistent generation of motions compatible with both a target design basis floor spectrum for acceleration sensitive systems and a generalized interstory drift for displacement sensitive systems as expected for a specified normalized building height. The testing protocol has been calibrated to induce/impose on acceleration/displacement sensitive nonstructural systems a number of rainflow cycles compatible with the number of rainflow cycles induced/imposed by the floor motions recorded in buildings during real earthquakes. Testing of a full-scale of a hospital emergency room with architectural finishes and medical equipment was used to demonstrate the capabilities of the UB-NCS and the suitability of the proposed testing protocol for assessing the seismic performance of combined displacement-acceleration nonstructural systems. The experiments successfully verified the testing capabilities of the UB-NCS to reproduce, in a controlled environment, the full-scale floor motions generating damage levels compatible with the damage levels observed in multistory building during seismic events.

REFERENCES

Cartwright, D.E., and Longuet-Higgins, M.S. (1956). The Statistical Distribution of the Maxima of a Random Function. *Proceedings of the Royal Soc. of London. Series A, Math. and Physical Scs*. **237**(1209): p. 212-232.

Chopra, A.K., and Chintanapakdee, C. (2001). Drift Spectrum vs. Modal Analysis of Structural Response to Near-Fault Ground Motions. *Earthquake Spectra*. **17**(2): p. 221-234.

Gupta, I.D., and Trifunac, M.D. (1998). Defining Equivalent Stationary PSDF to Account for Nonstationarity of Earthquake Ground Motion. *Soil Dynamics and Earthquake Engineering*. **17**(2): p. 89-99.

Iwan, W.D. (1997). Drift Spectrum: Measure on Demand for Earthquake Ground Motions. *Journal of Structural Engineering*. **123**(4): p. 397-404.

Kim, J., and Collins, K.R. (2002). Closer Look at the Drift Demand Spectrum. *J. of Str. Eng*.**128**(7):p942-945.

Krawinkler, H., Parisi, F., Ibarra, L., Ayoub, A., and Medina, R. (2000). CUREE-Caltech Woodframe Project Publication W-02: Development of a Testing Protocol for Wood Frame Structures. CUREE.

Lang, A., and Restrepo, J. (2006). Seismic Performance Evaluation of Gypsum Wallboard Partitions. *Proc. 8th US National Conference on Earthquake Engineering*. April 18-21, San Francisco, California.

McGavin, G., and Patrucco, H. (1994). Survey of Non Structural Damage to Healthcare Facilities in the January 17, 1994, Northridge Earthquake. HMC Group: Ontario, CA.

Miranda, E., and Akkar, S. (2006). Generalized Interstory Drift Spectrum. *J. of Str. Eng*. **132**(6):p.840-852.

Mosqueda, G., Retamales, R., Filiatrault, A., and Reinhorn, A. (2008). Testing Facility for Experimental Evaluation of Nonstructural Components under Full-Scale Floor Motions. *In J. of Structural Design of Tall and Special Buildings.* In press.

Retamales, R. (2008). New Experimental Capabilities and Loading Protocols for Seismic Fragility and Qualification of Nonstructural Components. PhD Dissertation submitted to the Department of Civil, Structural and Environmental Engineering, University at Buffalo, Buffalo, p. 348.

Taghavi, S., and Miranda, E. (2006). Seismic Demand Assessment on Acceleration-Sensitive Building Nonstructural Components. *Proceedings 8th US NCEE*. April 18-21, San Francisco, California.

Wanitkorkul, A. and Filiatrault, A. (2005). Simulation of Strong Ground Motions for Seismic Fragility Evaluation of Nonstructural Components in Hospitals. Report No. MCEER 05-0005. Multidisciplinary Center for Earthquake Engineering Research. University at Buffalo, State University of New York, Buffalo.

Wilcoski, J., Gambill, J.B., and Smith, S.J. (1997). The CERL Equipment Fragility and Protection Procedure (CEFAPP), USACERL Technical Report 97/58. U.S. Army Corps of Engineers.